

## A 2D/3D coupling method for transport calculation

Liu Zhouyu\*, Liang Liang, Cao Liangzhi, Wu Hongchun

School of Nuclear Science and Technology, Xi'an Jiaotong University, Xi'an Shaanxi 710049, China

**Abstract** - In this paper a 2D/3D coupling method is developed, in which, the 3D SN solver is employed to get the axial leakage for the 2D radial calculation, while the 2D MOC solver calculates the homogeneous cross section and the correction factor for the 3D SN calculation. Iterations between 2D and 3D calculations are needed to get the converged results. The detailed theory of this 2D/3D coupling method is firstly introduced, including the derivation of the radial equation, the definition of the correction factor, and the expression of the averaged angular flux with the correction factor, then the impact of axial leakage to the MOC calculation results is simply analyzed. Finally the results for the 3D C5G7 problems are given to demonstrate the performance of the 2D/1D coupling method.

### I. INTRODUCTION

Nowadays the 2D/1D fusion method (2D/1D method) is becoming a standard transport method for whole-core calculations, and a lot of 2D/1D codes have been developed, such as CRX-3D<sup>[1,2]</sup>, DeCART<sup>[3,4]</sup>, nTRACER<sup>[5]</sup>, CHAPLET-3D<sup>[6]</sup>, AGENT<sup>[7]</sup>, TOMMOC<sup>[8]</sup>, Tiger-3D<sup>[9]</sup>, MPACT<sup>[10,11]</sup>, etc. The 2D/1D fusion method is coupled by the leakage term, and converged through the leakage iteration between the 2D MOC calculation and 1D calculation. Mitchell T.H. Young<sup>[12]</sup> coupled the 2D MOC to the 3D Sn solver, in which the 2D MOC provide the radial correction factors for the 3D calculations. But 3D calculation isn't coupled to the 2D MOC, which means no axial leakage is considered for the 2D MOC calculations. According to our previous analysis<sup>[13]</sup>, if the proper axial leakage is provided, the 2D MOC calculations with axial leakage will get reasonable results including  $k_{\text{eff}}$  and flux. Therefore, in this paper a 2D/3D coupling method is introduced, which is iteratively converged through the leakage term. The 3D S<sub>N</sub> solver calculates the axial leakage for the 2D MOC solver, while the 2D MOC solver provides the cross sections and the correction factor for the 3D S<sub>N</sub> solver.

### II. DESCRIPTION OF THE ACTUAL WORK

In this paper a 2D/3D coupling method is developed, in which, the 3D S<sub>N</sub> solver is employed to get the axial leakage for the 2D radial calculation, while the 2D MOC solver calculates the homogeneous cross section and the correction factor for the 3D S<sub>N</sub> calculation. Iterations between 2D and 3D calculations are needed to get the converged results.

In this paper, the detailed theory of this 2D/3D coupling method is firstly introduced, including the derivation of the radial equation, the definition of the correction factor, and the expression of the averaged angular flux with the

correction factor, then the impact of axial leakage to the MOC calculation results is simply analyzed. Finally the results for the 3D C5G7 problems are given to demonstrate the performance of the 2D/1D coupling method.

#### 1. Theory of the 2D/3D coupling method

Firstly, we start here with the original 3D multi-group transport equation written as Eq.(1):

$$\xi_m \frac{\partial \psi_g(\mathbf{r}, \Omega_m)}{\partial x} + \eta_m \frac{\partial \psi_g(\mathbf{r}, \Omega_m)}{\partial y} + \mu_m \frac{\partial \psi_g(\mathbf{r}, \Omega_m)}{\partial z} + \Sigma_{t,g}(\mathbf{r}) \psi_g(\mathbf{r}, \Omega_m) = Q_g(\mathbf{r}, \Omega_m) \quad (1)$$

where:

$$Q_g(\mathbf{r}) = \frac{\chi_g}{4\pi k_{\text{eff}}} \sum_{g'=1}^G (v\Sigma_f)_{g'}(\mathbf{r}) \phi_{g'}(\mathbf{r}) + \frac{1}{4\pi} \sum_{g'=1}^G \Sigma_{s0,g'-g}(\mathbf{r}) \phi_{g'}(\mathbf{r})$$

The radial 2D equation is obtained by integrating Eq.(1) over z-direction intervals:

$$\frac{1}{\Delta z_k} \int_{z_{k-1/2}}^{z_{k+1/2}} \left( \xi_m \frac{\partial \psi_g(\mathbf{r}, \Omega_m)}{\partial x} + \eta_m \frac{\partial \psi_g(\mathbf{r}, \Omega_m)}{\partial y} + \mu_m \frac{\partial \psi_g(\mathbf{r}, \Omega_m)}{\partial z} + \Sigma_{t,g}(\mathbf{r}) \psi_g(\mathbf{r}, \Omega_m) \right) dz = \frac{1}{\Delta z_k} \int_{z_{k-1/2}}^{z_{k+1/2}} Q_g(\mathbf{r}, \Omega_m) dz$$

It can be rewritten:

$$\xi_m \frac{\partial \psi_{g,m,k}(x,y)}{\partial x} + \eta_m \frac{\partial \psi_{g,m,k}(x,y)}{\partial y} + \Sigma_{t,g,k}(x,y) \psi_{g,m,k}(x,y) = Q_{g,k}(x,y) - TL_{g,m,k}^{\text{Axial}}(x,y) \quad (2)$$

Where:

$$TL_{g,m,k}^{\text{Axial}}(x,y) = \frac{\mu_m}{\Delta z_k} \left[ \psi_{g,m,k+1/2}(x,y) - \psi_{g,m,k-1/2}(x,y) \right]$$

The MOC method is used to solve the radial 2D equation. The right hand side of Eq.(2) is different from the original MOC equation because of the leakage term, which is determined by the 3D S<sub>N</sub> calculation. Since the general S<sub>N</sub>

Corresponding author:  
Liu Zhouyu, liuzhouyu1985@Hotmail.com

method is mostly applied to the structured geometries, and each pin is square in PWR and BWR, it is reasonable to get the 3D equation by integrating Eq.(1) over each pin:

$$\frac{1}{\Delta x \Delta y} \int_{y_{i-1/2}}^{y_{i+1/2}} \int_{x_{i-1/2}}^{x_{i+1/2}} \left[ \xi_m \frac{\partial \psi_g(\mathbf{r}, \Omega_m)}{\partial x} + \eta_m \frac{\partial \psi_g(\mathbf{r}, \Omega_m)}{\partial y} + \mu_m \frac{\partial \psi_g(\mathbf{r}, \Omega_m)}{\partial z} + \Sigma_{t,g}(\mathbf{r}) \psi_g(\mathbf{r}, \Omega_m) \right] dx dy = \frac{1}{\Delta x \Delta y} \int_{y_{i-1/2}}^{y_{i+1/2}} \int_{x_{i-1/2}}^{x_{i+1/2}} Q_g(\mathbf{r}, \Omega_m) dx dy$$

Rewriting the equation, the 3D  $S_N$  equation based on the pin mesh is

$$\xi_m \frac{\partial \psi_{g,m}^p}{\partial x} + \eta_m \frac{\partial \psi_{g,m}^p}{\partial y} + \mu_m \frac{\partial \psi_{g,m}^p}{\partial z} + \Sigma_{t,g,p} \psi_{g,m}^p = Q_g^p \quad (3)$$

Where:

$$\Sigma_{t,g,p} = \frac{\sum_{r \in P} \psi_{g,m}(r) * \Sigma_{t,g}(r) * V(r)}{\sum_{r \in P} \psi_{g,m}(r) * V(r)}$$

$$\psi_{g,m}^p = \frac{1}{\Delta x \Delta y} \int_{\Delta x \Delta y} \psi_{g,m}(x, y) dx dy$$

$$Q_{g,m}^p = \frac{1}{\Delta x \Delta y} \int_{\Delta x \Delta y} Q_{g,m}(x, y) dx dy$$

Here, the finite difference method is applied to solve the 3D  $S_N$  equation:

$$\xi_m \frac{\psi_{g,m,i+}^p - \psi_{g,m,i-}^p}{\Delta x} + \eta_m \frac{\psi_{g,m,j+}^p - \psi_{g,m,j-}^p}{\Delta y} + \mu_m \frac{\psi_{g,m,k+}^p - \psi_{g,m,k-}^p}{\Delta z} + \Sigma_{t,g,p} \psi_{g,m}^p = Q_g^p \quad (4)$$

Assuming the averaged angular flux is equal to the average of the incoming flux and the outgoing flux:

$$\psi_{g,m}^p = (\psi_{g,m,a+}^p + \psi_{g,m,a-}^p) / 2 \quad (a = i, j, k) \quad (5)$$

The expression of the average angular flux is obtained by:

$$\psi_{g,m}^p = \frac{Q_g^p + 2\left(\frac{\mu_m}{\Delta x} \psi_{g,m,i-}^p + \frac{\eta_m}{\Delta y} \psi_{g,m,j-}^p + \frac{\varepsilon_m}{\Delta z} \psi_{g,m,k-}^p\right)}{2\left(\frac{\mu_m}{\Delta x} + \frac{\eta_m}{\Delta y} + \frac{\varepsilon_m}{\Delta z}\right) + \Sigma_{t,g,p}} \quad (6)$$

The correction factor is introduced to maintain the relationship of the incoming and outgoing fluxes same with that of the MOC solver.

$$\psi_{g,m}^p = (1/2 + \alpha_l)(\psi_{g,m,l+}^p + \psi_{g,m,l-}^p) \quad (7)$$

$$\psi_{g,m,l+}^p = \frac{\psi_{g,m}^p}{(1/2 + \alpha_l)} - \psi_{g,m,l-}^p$$

So the average angular flux is expressed in Eq.(8):

$$\psi_{g,m}^p = \frac{Q_g^p + 2\left(\frac{\mu_m}{\Delta x} \psi_{g,m,i-}^p + \frac{\eta_m}{\Delta y} \psi_{g,m,j-}^p + \frac{\varepsilon_m}{\Delta z} \psi_{g,m,k-}^p\right)}{\frac{\mu_m}{\Delta x(1/2 + \alpha_i)} + \frac{\eta_m}{\Delta y(1/2 + \alpha_j)} + 2\frac{\varepsilon_m}{\Delta z} + \Sigma_{t,g,p}} \quad (8)$$

The correction factor is to preserve the 3D  $S_N$  results to the 2D MOC solver.

$$\alpha_l = \frac{\psi_{g,m}^{p,moc}}{(\psi_{g,m,l+}^{p,moc} + \psi_{g,m,l-}^{p,moc})} - 1/2 \quad l = i, j \quad (9)$$

The homogeneous cross sections and the correction factor are iteratively updated by previous 2D calculations. And the iteration between the 2D MOC and the 3D  $S_N$  calculations is performed until the eigenvalue and scalar flux are converged. The calculation flow is show as Fig. 1.

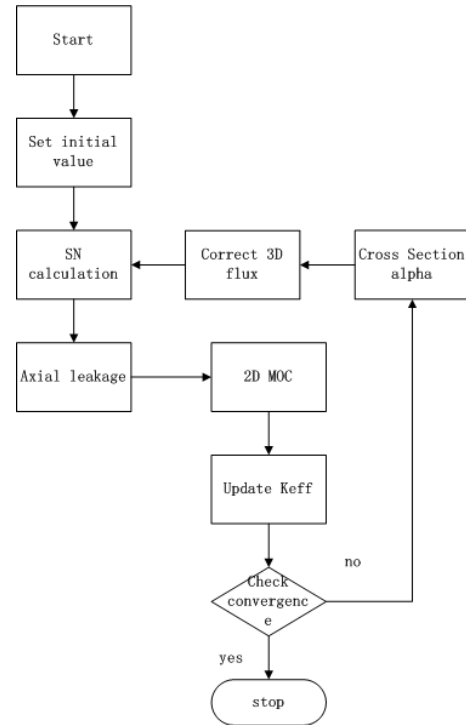


Fig.1 calculation flow chart of the coupling method

## 2. Analysis of the axial leakage

For the plane  $k$  the 2D equation is:

$$\Delta z_k \left[ \xi_m \frac{\partial \psi_{g,m,k}(x, y)}{\partial x} + \eta_m \frac{\partial \psi_{g,m,k}(x, y)}{\partial y} + \Sigma_{t,g,k}(x, y) \psi_{g,m,k}(x, y) \right] = \Delta z_k Q_{g,k}(x, y) - \mu_m [\psi_{g,m,k+1/2}(x, y) - \psi_{g,m,k-1/2}(x, y)] \quad (10)$$

From the Eq.(10), it can be found that the error of integral flux for the 2D calculation depends on the leakage term

which is determined by the difference between the top and bottom surface angular flux. The same conclusion can also be drawn for plane  $k+1$ :

$$\Delta z_{k+1} \left[ \begin{array}{l} \xi_m \frac{\partial \psi_{g,m,k+1}(x,y)}{\partial x} + \eta_m \frac{\partial \psi_{g,m,k+1}(x,y)}{\partial y} \\ + \sum_{t,g,k+1}(x,y) \psi_{g,m,k+1}(x,y) \end{array} \right] \quad (11)$$

$$= \Delta z_{k+1} Q_{g,k+1}(x,y) - \mu_m \left[ \psi_{g,m,k+3/2}(x,y) - \psi_{g,m,k+1/2}(x,y) \right]$$

Assuming that the total cross section of plane  $k$  to be equal to that of plane  $k+1$ , then summing up Eq.(11) and Eq.(12), the surface angular flux of the  $k+1/2$  surface on the right hand side will be eliminated as shown in Eq.(13).

$$\xi_m \frac{\partial (\Delta z_k \psi_{g,m,k}(x,y) + \Delta z_{k+1} \psi_{g,m,k+1}(x,y))}{\partial x} + \eta_m \frac{\partial (\Delta z_k \psi_{g,m,k}(x,y) + \Delta z_{k+1} \psi_{g,m,k+1}(x,y))}{\partial y} \quad (13)$$

$$+ \sum_{t,g,k}(x,y) (\Delta z_k \psi_{g,m,k}(x,y) + \Delta z_{k+1} \psi_{g,m,k+1}(x,y))$$

$$= (\Delta z_k Q_{g,k+1}(x,y) + \Delta z_{k+1} Q_{g,k+1}(x,y))$$

$$- \mu_m \left[ \psi_{g,m,k+3/2}(x,y) - \psi_{g,m,k-1/2}(x,y) \right]$$

Where:

$\psi_{g,m,k+3/2}(x,y)$  is the top surface angular flux

$\psi_{g,m,k-1/2}(x,y)$  is the bottom surface angular flux

$\Delta z_k \psi_{g,m,k}(x,y) + \Delta z_{k+1} \psi_{g,m,k+1}(x,y)$  is the integrated angular flux of plane  $k$  and plane  $k+1$ .

If the top surface angular flux and bottom surface angular flux are known, the integrated angular flux of plane  $k$  and plane  $k+1$  (solutions of Eq.(11). Eq.(12)) can be obtained by integrating Eq.错误!未找到引用源。 over the plane  $k$  and plane  $k+1$ .

$$\xi_m \frac{\partial ((\Delta z_{k+1} + \Delta z_k) \psi_{g,m,(k,k+1)}(x,y))}{\partial x} + \eta_m \frac{\partial ((\Delta z_{k+1} + \Delta z_k) \psi_{g,m,(k,k+1)}(x,y))}{\partial y} \quad (14)$$

$$+ \sum_{t,g,(k,k+1)}(x,y) ((\Delta z_{k+1} + \Delta z_k) \psi_{g,m,(k,k+1)}(x,y))$$

$$= (\Delta z_{k+1} + \Delta z_k) Q_{g,(k,k+1)}(x,y)$$

$$- \mu_m \left[ \psi_{g,m,k+3/2}(x,y) - \psi_{g,m,k-1/2}(x,y) \right]$$

where,  $\psi_{g,m,(k,k+1)}$  is the average angular flux of plane  $k$  and plane  $k+1$ .

Comparing Eq.(13) with Eq.(14), it can be found that if the axial surface angular fluxes

$\psi_{g,m,k+3/2}(x,y), \psi_{g,m,k+1/2}(x,y), \psi_{g,m,k-1/2}(x,y)$  is

known, the solution of Eq.(13) is equal to the solution of Eq.(14).

$$\psi_{g,m,(k,k+1)} = \frac{\Delta z_k \psi_{g,m,k}(x,y) + \Delta z_{k+1} \psi_{g,m,k+1}(x,y)}{\Delta z_k + \Delta z_{k+1}} \quad (15)$$

It is indicated that there is no need to solve the 2D MOC twice for plane  $k$  and plane  $k+1$ , when the distribution of the axial leakage for every plane is known, the accurate integral flux can be obtained no matter how large the axial plane for the 2D calculation is.

In the 2D/3D coupling method, the 3D  $S_N$  solver is to calculate the axial leakage for 2D MOC solver, while the 2D MOC calculations is supplying the cross section and the correction factor for the 3D  $S_N$  solver. The new 2D/3D coupling method is implemented in the reactor physics code NECP-X.

### 3. Numerical results

The C5G7 benchmark is designed to test the ability of modern deterministic transport methods and codes to treat reactor problems The extension of the 3-D calculations was proposed in May 2003 to provide a more challenging test of present day three-dimensional methods' ability to handle spatial homogeneities. The reactor core size was decreased to allow the calculations to be carried out within the limitations of present-day computers. Control rods were introduced to increase the heterogeneity of the problems. The arrangement of the benchmark is shown in Fig.2 – Fig. 7.

The calculation parameter is as below:

1) The core is divided into 4 layers to process 2D MOC calculation

- 2) The mesh size of xy direction of 3D Sn calculation is 1.26 cm, same as the size of each pin. The mesh size of z direction is 1.0 cm which is finer than the size of MOC calculation layer.
- 3) The ray spacing in 2D MOC is 0.03 cm.
- 4) There are 4 polar angles and 6 azimuthal angles in one octant.
- 5) The criteria of the keff and flux is 1.0E-6 and 1.0E-5.

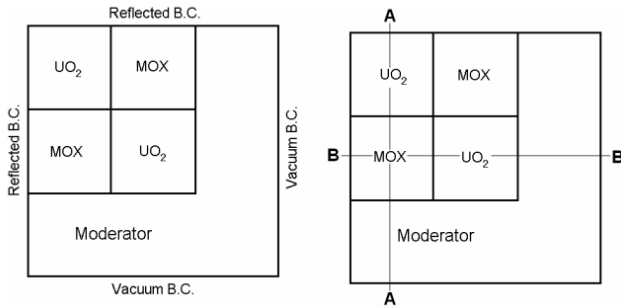


Fig.2 The radial geometry of the C5G7 benchmark

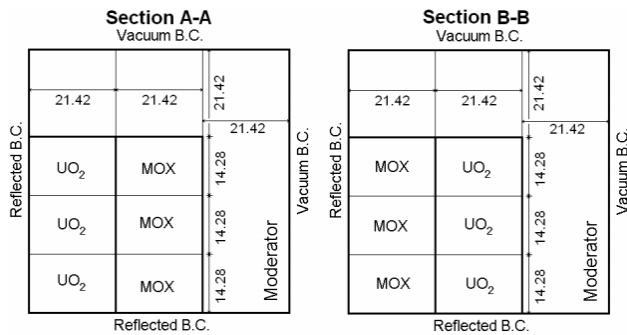


Fig.3 The axial geometry of the C5G7 benchmark

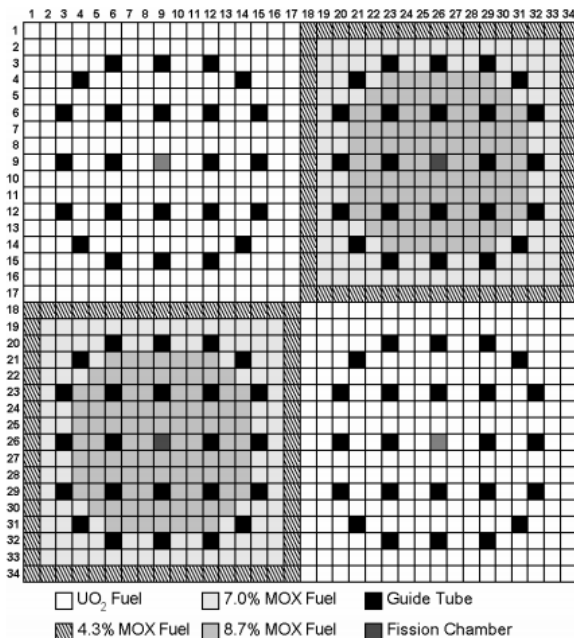


Fig 4 The pin arrangement of the C5G7 benchmark

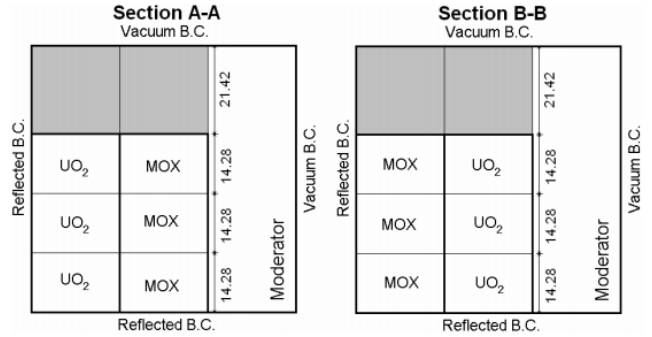


Fig. 5 Three-dimensional geometry for the Unrodded configuration

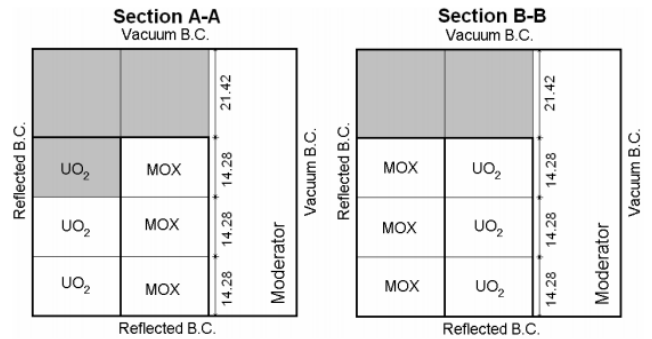


Fig. 6 Three-dimensional geometry for the Rodded A configuration

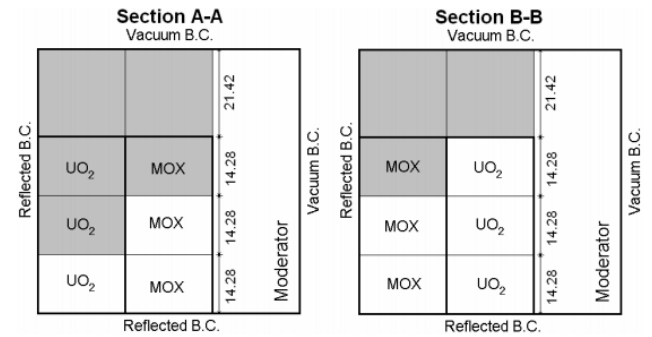


Fig. 7 Three-dimensional geometry for the Rodded B configuration

The numerical results of the benchmark are shown in Table 1 – Table 3. The  $k_{eff}$  of each case is close to the reference while the relative error is less than 50 pcm. The overall pin power agrees very well, including the maximum pin power and the lattice power.

For the unrodded case, the relative error of the maximum pin power of slice 3 is less than 1.5% while the relative error of each lattice power of slice 3 is less than 1.2%, the distribution of the relative error of pin power is shown in Fig. 8, which suggest that this coupling method can get a accurate eigenvalue and pin power distribution.

Table 1 The result of unrodded case

Unrodded	Reference MCNP	NECP-X_2D3D	Relative error(%)	slice 3			
Keff	1.14308	1.1432	-0.01	Max rod power	0.304	0.299	1.64
Max rod power	2.481	2.477	0.16	Inner U02lattice	56.3	55	2.31
Inner U02lattice	491.2	490.4	0.16	MOX lattice	39.2	38.6	1.53
MOX lattice	212.7	213	-0.14	Outer U02 lattice	28.2	27.9	1.06
Outer U02 lattice	139.4	139.6	-0.14				
slice 1							
Max rod power	1.108	1.113	-0.45				
Inner U02lattice	219	220.1	-0.5				
MOX lattice	94.5	95.7	-1.27				
Outer U02 lattice	62.1	62.8	-1.13				
slice 2							
Max rod power	0.882	0.879	0.34				
Inner U02lattice	174.2	175.4	-0.69				
MOX lattice	75.2	74.8	0.53				
Outer U02 lattice	49.5	49.2	0.61				
slice 3							
Max rod power	0.491	0.484	1.43				
Inner U02lattice	97.9	96.8	1.12				
MOX lattice	42.9	42.5	0.93				
Outer U02 lattice	27.8	27.5	1.08				

For the rodded A case, the relative error of the maximum pin power of slice 3 is less than 2.0% while the relative error of each lattice power of slice 3 is less than 2.4%. The distribution of the relative error of pin power is shown in Fig. 9.

Table 2 The result of rodded A case

rodded A	Reference MCNP	NECP-X_2D3D	Relative error(%)
Keff	1.128	1.1285	-0.04
Max rod power	2.253	2.252	0.04
Inner U02lattice	461.2	460.9	0.07
MOX lattice	221.7	221.8	-0.05
Outer U02 lattice	151.4	151.6	-0.13
slice 1			
Max rod power	1.197	1.203	-0.5
Inner U02lattice	237.4	239	-0.67
MOX lattice	104.5	105.8	-1.24
Outer U02 lattice	69.8	70.7	-1.29
slice 2			
Max rod power	0.832	0.83	0.24
Inner U02lattice	167.5	166.8	0.42
MOX lattice	78	77.3	0.9
Outer U02 lattice	53.4	53	0.75

For the rodded B case, the relative error of the maximum pin power of slice 3 is less than 3.5% while the relative error of each lattice power of slice 3 is less than 3.0%. The distribution of the relative error of pin power is shown in Fig. 10. The result of the rodded B case calculated by the 2D/1D code with the same calculation parameter is shown in Table 4. According to Table 4, it is obvious that the 2D/3D method is more precise than 2D/1D method with coarser MOC layer.

Table 3 The result of rodded B case

Rodded B	ref	NECP-X_2D3D	err/%
Keff	1.0777	1.07829	-0.05
max rod power	1.835	1.835	0.01
U02_inside	395.4	395.3	0.03
MOX	236.6	236.7	-0.04
U02_outside	187.3	187.5	-0.11
slice 1			
max rod power	1.2	1.211	-0.92
U02_inside	247.7	250.1	-0.97
MOX	125.8	127.5	-1.35
U02_outside	91.6	92.8	-1.31
slice 2			
max rod power	0.554	0.548	1.08
U02_inside	106.6	105.1	1.41
MOX	81.4	80.4	1.23
U02_outside	65	64.5	0.77
slice 3			
max rod power	0.217	0.21	3.23
U02_inside	41.1	40	2.68
MOX	29.4	28.8	2.04
U02_outside	30.7	30.2	1.63

Table 4 The result of rodded B case calculated by 2D1D method

Rodded B	ref	NECP-X_2D1D	err/%
Keff	1.0777	1.08191	-0.39
max rod power	1.835	1.851	-0.87
U02_inside	395.4	398.3	-0.73
MOX	236.6	235.9	0.3

U02_outside	187.3	185.8	0.8
slice 1			
max rod power	1.2	1.24	-3.33
U02_inside	247.7	253.9	-2.5
MOX	125.8	125.4	0.32
U02_outside	91.6	90.6	1.09
slice 2			
max rod power	0.554	0.558	-0.72
U02_inside	106.6	106.2	0.38
MOX	81.4	81.5	-0.12
U02_outside	65	64.7	0.46
slice 3			
max rod power	0.217	0.198	8.76
U02_inside	41.1	38.2	7.06
MOX	29.4	29.1	1.02
U02_outside	30.7	30.5	0.65

the size of the MOC layer is smaller, the converged result can't be obtained. The undergoing work is to improve the stability of this method.

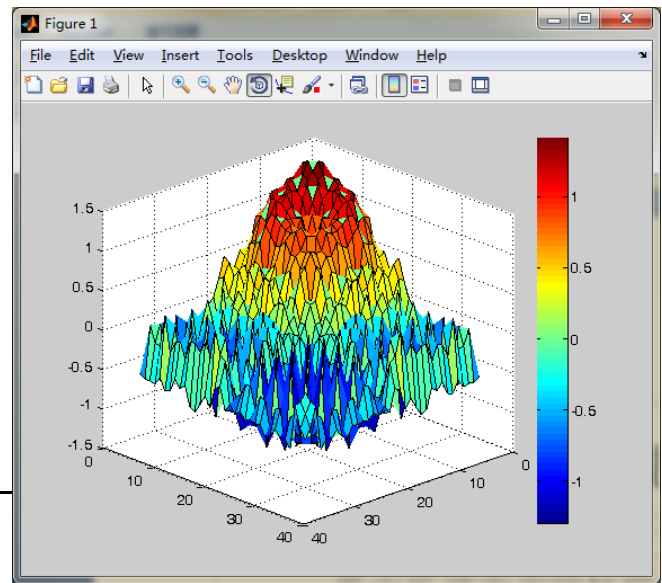


Fig 9 The distribution of the relative error of pin power of rodA case

Considering all the numerical result of each case, the  $k_{eff}$  and the overall pin power agree well with the reference result from Monte Carlo code.

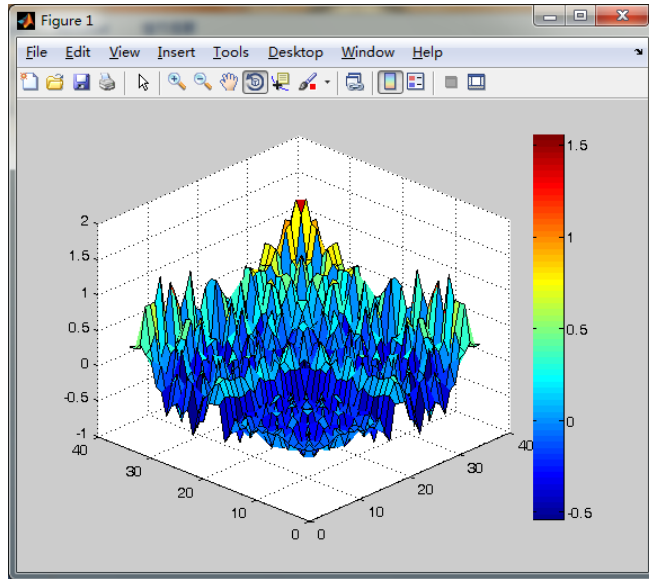


Fig 8 The distribution of the relative error of pin power of unrodded case

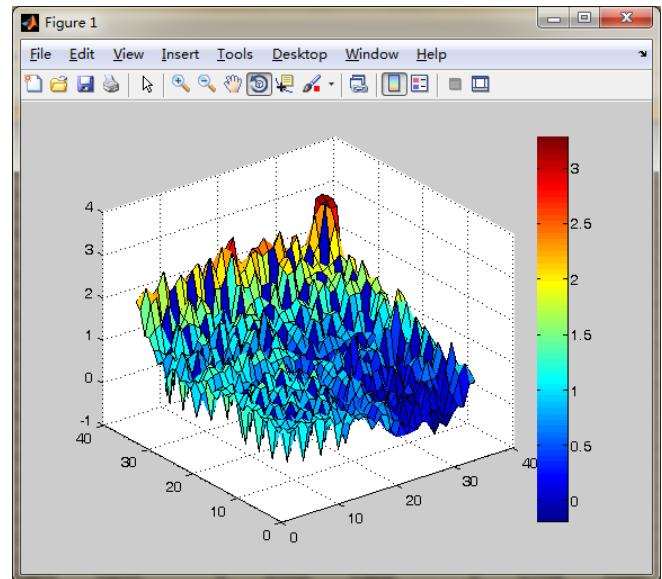


Fig 10 The distribution of the relative error of pin power of rodB case

#### 4. CONCLUSION

In this study, an iteration version of the 2D/3D coupling method is introduced and the numerical result of C5G7 3D extension is demonstrated. The numerical result indicates that this coupling method can obtain accurate eigenvalue and pin power distribution. Compared with the result of 2D/1D method, the  $k_{eff}$  and the pin power distribution are both better with coarser MOC layer. Currently, this method still has some stability issue. When

#### ACKNOWLEDGE

This research was financially supported by the National Natural Science Foundation of China (Approved numbers 11545015 and 11522544).

#### REFERENCES

1. Cho N Z, Lee G S, Park C J. Fusion of Method of Characteristics and Nodal Method for 3-D Whole-Core Transport Calculation. Transactions of the American Nuclear Society, 2002, 87:322-324.
2. Gil Soo Lee, N Z C. 2D/1D fusion method solutions of the three-dimensional transport OECD benchmark problem C5G7 MOX. Progress in Nuclear Energy, 2006,48:410-423.
3. Joo H G, Cho J Y, Kim K S, et al. Methods and performance of a three-dimensional whole-core transport code DeCART. PHYSOR 2004, The Physics of Fuel Cycles and Advanced Nuclear Systems - Global Developments, April 25, 2004 - April 29, 2004, Chicago, IL, United states, 2004[C]. American Nuclear Society.
4. Jin Young Cho, H G J. Solution of the C5G7MOX benchmark three-dimensional extension problems by the DeCART direct whole core calculation code. Progress in Nuclear Energy, 2006, 48:456-466.
5. Jung Y S, Shim C B, Lim C H, et al. Practical numerical reactor employing direct whole core neutron transport and subchannel thermal/hydraulic solvers. ANNALS OF NUCLEAR ENERGY, 2013,62:357-374.
6. Kosaka S. 3-D extension C5G7 MOX benchmark results using CHAPLET-3D. Progress in Nuclear Energy, 2006,48:439-444.
7. Xiao S. Hardware Accelerated High Performance Neutron Transport Computation Based on AGENT Methodology[D]. West Lafayette, Indiana, United States: Purdue University, 2009.
8. Zhang H, Zheng Y, Wu H, et al. A 2D/1D coupling neutron transport method based on the matrix MOC and NEM methods. International Conference on Mathematics and Computational Methods Applied to Nuclear Science & Engineering(M&C 2013), Sun Valley, ID, United states, 2013[C]. American Nuclear Society.
9. Wu Wenbin. Research on 2D/1D Coupled 3D Whole-core Transport Calculations Based on Parallel Computation[D]. Tsinghua University, 2014.
10. Kelley B W, Larsen E W. 2D/1D approximations to the 3D neutron transport equation. I: Theory, International Conference on Mathematics and Computational Methods Applied to Nuclear Science & Engineering(M&C 2013), Sun Valley, ID, United states, 2013[C]. American Nuclear Society.
11. Kelley B W, Collins B, Larsen E W. 2D/1D approximations to the 3d neutron transport equation. II: Numerical comparisons, International Conference on Mathematics and Computational Methods Applied to Nuclear Science & Engineering(M&C 2013), Sun Valley, ID, United states, 2013[C]. American Nuclear Society.
12. Mitchell T.H. Young, Benjamin Collins, William Martin. 2-D/3-D Coupling Between the Method of Characteristics and Discrete Ordinates, Transactions of the American Nuclear Society, Vol. 109, Washington, D.C., November 10–14, 2013.
13. Liang Liang, Zhouyu Liu, Youqi Zheng, Liangzhi Cao, Hongchun Wu, Leakage reconstruction method for 2D/1D fusion transport calculations, Progress in Nuclear Energy, Volume 97, May 2017, Pages 60-73, ISSN 0149-1970, <http://dx.doi.org/10.1016/j.pnucene.2016.12.016>.